

Synthesis, crystal structure and photocatalytic properties of an unprecedented arsenic-disubstituted Lindqvist-type peroxopolyoxoniobate ion: $\{\text{As}_2\text{Nb}_4(\text{O}_2)_4\text{O}_{14}\text{H}_{1.5}\}^{4.5-}$ †

Cite this: *Dalton Trans.*, 2014, **43**, 9843

Received 24th March 2014,
Accepted 29th April 2014

DOI: 10.1039/c4dt00875h

www.rsc.org/dalton

Qiaohua Geng, Qisen Liu, Pengtao Ma, Jingping Wang* and Jingyang Niu*

An unprecedented arsenic-disubstituted Lindqvist-type peroxopolyoxoniobate $\text{Cs}_{2.5}\text{Na}_2\{\text{As}_2\text{Nb}_4(\text{O}_2)_4\text{O}_{14}\text{H}_{1.5}\}\cdot 11\text{H}_2\text{O}$ has been successfully synthesized and characterized. The photocatalytic activity of the cluster for H_2 evolution from water is investigated by irradiating with a 300 W Xe lamp, which shows a certain photocatalytic water splitting activity.

Polyoxoniobates (PONs) have attracted significant interest not only for the relatively limited structural diversity reported, but also for their significant potential application in different areas, such as virology, nuclear-waste treatment, and the base-catalyzed decomposition of biocontaminants.¹ Although the synthetic conditions of PONs are more difficult compared with the larger classes of polyoxometalate based on W, Mo or V, the number of substituted niobates known to date has achieved great progress in the past ten years. Up to now, isopolyoxoniobates including $[\text{Nb}_6\text{O}_{19}]^{8-}$,² $[\text{Nb}_{10}\text{O}_{28}]^{6-}$,³ $[\text{Nb}_{20}\text{O}_{54}]^{8-}$,⁴ $[\text{H}_9\text{Nb}_{24}\text{O}_{72}]^{15-}$,⁵ $[\text{HNb}_{27}\text{O}_{76}]^{16-}$,^{6a} $[\text{H}_{10}\text{Nb}_{31}\text{O}_{93}(\text{CO}_3)]^{23-}$,^{6a} and $[\text{H}_{10}\text{Nb}_{32}\text{O}_{96}]^{4-}$ ^{6b} have been isolated in the literature. On the other hand, a number of transition-metal-substituted heteropolyoxoniobates have been reported, including Ti^{IV}-substituted PONs $[\text{Ti}_2\text{Nb}_8\text{O}_{28}]^{8-}$,^{7a} $[\text{TiNb}_9\text{O}_{28}]^{7-}$,^{7b} and $[\text{Ti}_{12}\text{Nb}_6\text{O}_{44}]^{10-}$.^{7c} The copper-substituted ion $[\text{CuNb}_{11}\text{O}_{35}\text{H}_4]^{9-}$,⁸ the vanadium-substituted ions $[\text{VNb}_{12}\text{O}_{40}(\text{VO})_2]^{9-}$,^{9a} $[\text{H}_6\text{V}_4\text{Nb}_6\text{O}_{30}]^{4-}$,^{9b} $[\text{Nb}_{10}\text{V}_4\text{O}_{40}(\text{OH})_2]^{12-}$,^{9c} and $[\text{V}_3\text{Nb}_{12}\text{O}_{42}]^{9-}$,^{9d} the chromium-substituted ion $[\text{Cr}_2(\text{OH})_4\text{Nb}_{10}\text{O}_{30}]^{8-}$,¹⁰ the iron-substituted ion $[\text{H}_2\text{Fe}^{\text{III}}\text{Nb}_9\text{O}_{28}]^{6-}$ ¹¹ and the nickel-substituted ion $[\text{H}_3\text{Ni}^{\text{II}}\text{Nb}_9\text{O}_{28}]^{6-}$ ¹¹ were also obtained. Furthermore, inspired by the work of Finke,^{12,13} Hill¹⁴ and their co-workers, the peroxopolyoxoniobates synthesized by the $[\text{Nb}_6\text{O}_{19}]^{8-}$ reaction in H_2O_2 solution are appropriate candidates for studying PONs in

acidic solution. Peroxide-ligated PONs have been isolated, including $[\text{Ti}_{12}\text{Nb}_6\text{O}_{38}(\text{O}_2)_6]^{10-}$ ¹⁵ and $[\text{H}_3\text{Nb}_6\text{O}_{13}(\text{O}_2)_6]^{5-}$,¹⁶ and so on. However, heterometal-substituted Lindqvist-type PONs have been relatively less explored and the only two examples of ions are the tungsten-rich $[\text{HNb}_2\text{W}_4\text{O}_{19}]^{3-}$ ¹⁷ and the tellurium-monosubstituted $[\text{H}_2\text{TeNb}_5\text{O}_{19}]^{5-}$.¹⁸ To date, both peroxide-ligated and heteroatom-substituted Lindqvist-type PONs have never been reported in the literature.

Herein, based on the previous work, we report the synthesis and structural characterization of an unprecedented arsenic-disubstituted Lindqvist-type peroxopolyoxoniobate $\text{Cs}_{2.5}\text{H}_{1.5}\text{Na}_2\{\text{As}_2\text{Nb}_4(\text{O}_2)_4\text{O}_{14}\}\cdot 11\text{H}_2\text{O}$ (**1**). To our knowledge, this compound represents the first example of integrating arsenic atoms into the peroxopolyoxoniobate.

Compound **1** was prepared by the reaction of $\text{K}_7\text{H}[\text{Nb}_6\text{O}_{19}]\cdot 13\text{H}_2\text{O}$,^{19,20} H_2O_2 , $\text{Na}_3\text{AsO}_4\cdot 12\text{H}_2\text{O}$, HCl and NaOH at 80 °C for 3 h. In the synthesis of compound **1**, parallel experiments show that several factors such as reactants, temperature, pH value and the concentration of the reaction system can influence the structure and extend structural diversity of the products. It is worth noting that crystals can only be obtained by the diffusion method and the best mixed solvent volume ratio of $\text{CH}_3\text{CH}_2\text{OH}-\text{H}_2\text{O}$ is 1 : 2.

The phase purity of **1** was characterized by the powder X-ray diffraction (PXRD) pattern of the bulk product. The PXRD pattern is in good agreement with the calculated pattern based on the result from single-crystal X-ray diffraction (Fig. S1†), which confirms that the phase is pure. The difference in intensity may be due to the preferred orientation of the powder samples. Single-crystal X-ray structural analysis shows that the structure of compound **1** possesses the cluster of $\{\text{As}_2\text{Nb}_4(\text{O}_2)_4\text{O}_{14}\text{H}_{1.5}\}^{4.5-}$ along with 1.5 protons, 2.5 Cs^+ cations and eleven water molecules with orthorhombic molecular symmetry, $Pnma$ space group.‡ In the novel cluster of $\{\text{As}_2\text{Nb}_4(\text{O}_2)_4\text{O}_{14}\text{H}_{1.5}\}^{4.5-}$, four Nb and two As atoms are connected to each other through bridging oxygen atoms (Fig. 1). Compared with the archetype Lindqvist-type structure of the $[\text{Nb}_6\text{O}_{19}]^{8-}$ ion, the cluster of **1** can be seen as two Nb atoms being replaced by the two As atoms. The angles of Nb–O_b–Nb,

Key Laboratory of Polyoxometalates Chemistry of Henan Province, Institute of Molecular and Crystal Engineering, College of Chemistry and Chemical Engineering, Henan University, Kaifeng 475004, China. E-mail: jpwang@henu.edu.cn, jyniu@henu.edu.cn; Fax: (+86) 371-23886876

† Electronic supplementary information (ESI) available: The experimental sections of **1**, XRPD spectra, bond valence sum calculations, IR spectra, UV spectra, the diffuse reflectance UV-vis-NIR spectra of K-M function vs. energy and TG analyses. See DOI: 10.1039/c4dt00875h

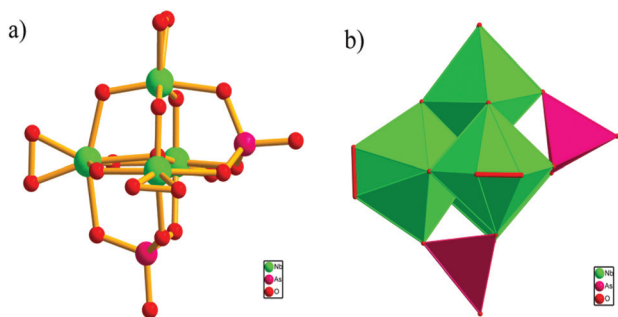


Fig. 1 (a) Ball-and-stick representation of the $\{As_2Nb_4(O_2)_4O_{14}\}^{6-}$ unit. (b) Polyhedral view of the $\{As_2Nb_4(O_2)_4O_{14}\}^{6-}$ cluster. The discrete Cs^+ , Na^+ cations and lattice water molecules are omitted for clarity.

Nb–O $_{\mu_4}$ –Nb are between 109.3(3) and 113.5(3) $^\circ$, 96.4(4) and 98.3(4) $^\circ$, and the bond lengths of Nb–O $_b$ and Nb– μ_4 –O are in the range of 1.875–2.095 Å and 2.106–2.273 Å, respectively. Notably, in the polyanion of **1**, all four terminal oxygen atoms of Nb atoms are replaced by η^2 -O $_2^{(1)2-}$ and the bond lengths of Nb–O $_2^{(1)2-}$ are between 1.951(7) and 1.979(9) Å which are longer than the Nb–O $_t$ (1.75–1.80 Å).²¹ And the average bond length of the four peroxo-containing bands is 1.47 Å which is comparable to that observed in the crystal structure of hydrogen peroxo (1.49 Å)²² and also similar to those in the peroxo groups in other reported POMs.^{14a-c,23,24} Interestingly, these atoms including Nb(2), Nb(3), As(1), As(2), O(7) are coplanar and can form a symmetry plane of the whole structure. The X-ray diffraction analyses also show that the Nb atoms here adopt a pseudo-octahedral configuration which is similar to that of the reported ion $[H_3Nb_6O_{13}(O_2)_6]^{5-}$,¹⁶ and the substituted arsenic atoms here adopt a tetrahedral geometry. The central As–O bond lengths range from 1.655(9) to 1.699(9) Å and the O–As–O angles are in the range of 106.6(5)–115.1(4) $^\circ$. The band valence sum (BVS) calculations²⁵ confirm that all the Nb and As atoms are in the +5 oxidation state [Scheme S1 \dagger]. Furthermore, the BVS calculations give the values of 1.35 and 1.36 for O $_{14}$ and O $_{15}$, respectively, which are relatively lower than those of other oxygen atoms in the framework (1.65–2.10) and further indicate the most possible sites for protonation. [The details are depicted in Fig. S2 and Schemes S2, S3.†]

The IR spectrum of compound **1** [Fig. S3 \dagger] is recorded between 400 and 4000 cm^{-1} with a KBr pellet, which is very useful for the identification of characteristic vibration bands in products. In the IR spectrum of compound **1**, the characteristic bands located at around 856 cm^{-1} and 853 cm^{-1} are assigned to the ν (As–O) and peroxo group ν (O–O) vibrations,²⁶ respectively, while the characteristic peaks in the range of 400–800 cm^{-1} are attributed to the ν (Nb–O $_b$ –Nb) vibrations.²⁷

The UV spectrum of compound **1** in aqueous solution displays two absorption bands centered at 200 nm and 280 nm, respectively. The higher energy band (200 nm) can be assigned to the O $_t$ →Nb charge transfer transition, whereas the lower one (280 nm) can be attributed to the charge transfer transition of O $_b$ →Nb, suggesting the presence of the polyoxoanion.

In order to investigate the stability of **1** in the aqueous solution, the *in situ* UV spectroscopic measurements were performed, and the systematic results revealed that **1** could stably exist at least for 24 h in the aqueous solution at ambient temperature [Fig. S4 \dagger].

It is well known that the PONs are commonly sensitive to the pH values of the media. Therefore, in order to investigate the influence of the pH values on the stability of **1** in aqueous solution, compound **1** has also been elaborately probed by means of UV spectra. Diluted HCl solution and NaOH solution were used to adjust the pH values in the acidic direction and the alkaline direction, respectively. The UV spectrum of compound **1** in aqueous solution displays two absorption bands at 200 and 280 nm, respectively, and the original pH value of it in water (5×10^{-5} mol L $^{-1}$) was 7.5 [Fig. S5 \dagger]. When the pH value gradually decreases to 2.0, the absorbance band at 280 nm shows a red-shift and disappears finally. While the other absorbance band at 200 nm shows a little blue-shift, which may be attributed to the decomposition of the cluster. The reason for the red-shift of the O $_t$ →Nb band may be related to the protonation of the terminal oxygen atoms of the polyoxoanion.^{28,29} In contrast, when the pH value of **1** gradually increases to 10.0, the absorption band at 280 nm shows a little blue-shift and becomes weaker and weaker until it vanishes, while the absorption band at 200 nm only becomes a little weaker than the initial state. All these changes suggest the decomposition of the **1** skeleton, and the results indicate that the skeleton of **1** can remain stable in the pH range of 4.0–8.0.

For the sake of studying the conductivity of **1**, the UV-vis diffuse reflectance spectrum of its powder sample was measured to obtain its band gaps (E_g), which was determined as the intersection point between the energy axis and the line extrapolated from the linear portion of the adsorption edge in a plot of the Kubelka–Munk function F against E . As is shown in Fig. S6,† the corresponding well-defined optical absorption associated with E_g can be assessed at 3.5 eV, which is smaller than the E_g of $K_7H[Nb_6O_{19}] \cdot 13H_2O$ [Fig. S7 \dagger], revealing the presence of an optical band gap and the nature of semi-conductivity with a wide band gap.

Thermal gravimetric analysis (TGA) was performed under a N $_2$ atmosphere from 25 to 800 $^\circ C$ [Fig. S8 \dagger]. The TG curve of **1** exhibits one slow step of weight loss, giving a total loss of 18.98% (calcd 18.97%) in the range of 25–800 $^\circ C$. The total weight loss can be assigned to the removal of eleven crystal water molecules, the dehydration of 1.5 protons and the loss of one oxygen atom in each peroxo group.

To explore the photocatalytic H $_2$ evolution activity of **1**, the experiments were performed in a quartz cell with 50 mL solution containing 50.0 mg sample of **1**, 10 mL CH $_3$ OH, 40 mL 0.5 M HCl, and 1.0 mL H $_2$ PtCl $_6$ solution (1.50 mg Pt).^{18,26b} The catalyst solution was irradiated under UV and visible light from a 300 W Xe lamp. Methanol was used as a sacrificial electron donor and H $_2$ was monitored by gas chromatography. The photocatalytic water splitting activity of $K_7H[Nb_6O_{19}] \cdot 13H_2O$ was also measured. As is shown in Fig. 2, the total evolved H $_2$ of **1** and $K_7H[Nb_6O_{19}] \cdot 13H_2O$ during 10 h were 98.8 and

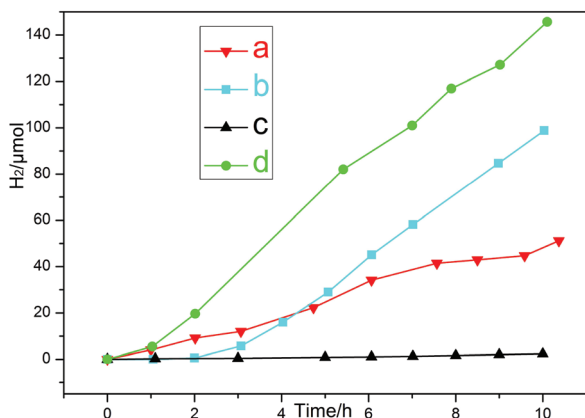


Fig. 2 Dependence of H_2 production on irradiation time with the use of compound **1** as a photocatalyst: (a) compound **1** in the presence of cobaloxime; (b) compound **1** in the solution of H_2PtCl_6 ; (c) the absence of compound **1** or $\text{K}_7\text{H}[\text{Nb}_6\text{O}_{19}]\cdot 13\text{H}_2\text{O}$; (d) $\text{K}_7\text{H}[\text{Nb}_6\text{O}_{19}]\cdot 13\text{H}_2\text{O}$ in the solution of H_2PtCl_6 .

145.7 μmol , and the H_2 evolution rates of them were 197.6 and 291.4 $\mu\text{mol g}^{-1} \text{h}^{-1}$, respectively. As a result, the effectivity of H_2 evolution activity from water of **1** was worse than that of $\text{K}_7\text{H}[\text{Nb}_6\text{O}_{19}]\cdot 13\text{H}_2\text{O}$, which suggests that Nb atoms play the main role in the process of photocatalytic H_2 evolution activity. After photocatalytic experiments, the PXRD pattern of **1** could not be obtained because of the smaller amount of the flocculent precipitate and the presence of the Pt cocatalyst. However, the FT-IR and UV-Vis spectra before and after the photocatalytic reactions have been given in ESI† to testify the stability of **1**. The results showed that the cluster of **1** has changed after the photocatalytic reactions, which means that the catalyst cannot be used repeatedly [Fig. S9, S10†].

In addition, we also explore the photocatalytic H_2 evolution activity with sample **1** as the UV light photosensitizer and catalyst, the Co^{III} (dmgH) 2pyCl complex as a cocatalyst and TEA as the sacrificial electron donor.^{6b,30} The experiments were performed in a quartz cell containing 50 mg (0.034 mM) sample, 50 mg (0.125 mmol) cobaloximes and 5 mL TEA in 45 mL of water (1/9 v/v). The catalyst solution was irradiated under UV and visible light from a 300 W Xe lamp. As shown in Fig. 2a, the total evolved H_2 during 10 h were 51.16 μmol and the H_2 evolution rate of compound **1** was 102.3, if using $\mu\text{mol g}^{-1} \text{h}^{-1}$ as the unit. Obviously, the photocatalytic H_2 evolution activity of compound **1** in the presence of the Pt cocatalyst was much better than in the system of cobaloxime as a cocatalyst.

Conclusions

In conclusion, an unprecedented arsenic-disubstituted Lindqvist-type peroxopolyoxoniobate based on the cluster of $\{\text{As}_2\text{Nb}_4(\text{O}_2)_4\text{O}_{14}\text{H}_{1.5}\}^{4.5-}$ has been successfully synthesized and characterized, and its photocatalytic H_2 evolution activity was also explored. The successful preparation of compound **1** not only provides us with a possible strategy to develop un-

expectedly PON derivatives by using the diffusion method, but also enriches the structural diversity of heteroatom-substituted Lindqvist-type peroxopolyoxoniobates. Currently, we are planning to systematically investigate the influence of the synthetic variables of the experiment procedure on the final products, as well as the photocatalytic H_2 evolution activity of their properties.

This work was supported by the Natural Science Foundation of China, the Special Research Fund for the Doctoral Program of Higher Education, Innovation Scientists and Technicians Troop Construction Projects of Henan Province and the Natural Science Foundation of Henan Province.

Notes and references

† Crystal data for **1**: CSD 427505. $M_r = 1452$, orthorhombic, space group $Pnma$, $a = 17.680(5) \text{ \AA}$, $b = 13.346(4) \text{ \AA}$, $c = 26.399(8) \text{ \AA}$, $V = 6229.3(13) \text{ \AA}^3$, $Z = 4$, $\mu = 6.566 \text{ mm}^{-1}$, $F(000) = 5528$, $\text{GOOF} = 1.073$. Of 30 869 total reflections collected, 5707 reflections are unique ($R_{\text{int}} = 0.0487$). $R_1 = 0.0513$, $wR_2 = 0.1610$ for 457 parameters and 5707 reflections [$I > 2\sigma(I)$].

- (a) J. T. Rhule, C. L. Hill and D. A. Judd, *Chem. Rev.*, 1998, **98**, 327–357; (b) A. V. Besserguenev, M. H. Dickman and M. T. Pope, *Inorg. Chem.*, 2001, **40**, 2582–2586; (c) M. H. Chiang, C. W. Williams, L. Soderholm and M. R. Antonio, *Eur. J. Inorg. Chem.*, 2003, **14**, 2663–2669; (d) F. Bonhomme, J. P. Larentzos, T. M. Alam, E. J. Maginn and M. Myman, *Inorg. Chem.*, 2005, **44**, 1774–1785; (e) A. J. Russell, J. A. Berberich, G. F. Drevon and R. R. Koepsel, *Annu. Rev. Biomed. Eng.*, 2003, **5**, 1–27; (f) M. Nyman, C. R. Powers, F. Bonhomme, T. M. Alam, E. J. Maginn and D. T. Hobbs, *Chem. Mater.*, 2008, **20**, 2513–2521.
- (a) K. Wassermann, M. H. Dickman and M. T. Pope, *Angew. Chem., Int. Ed.*, 1997, **36**, 1445–1448; (b) A. P. Muller and K. C. Kuhlmann, *Chem. Commun.*, 1999, 1347–1358; (c) I. Lindqvist, *Ark. Kemi*, 1953, **5**, 247–250.
- E. J. Graeber and B. Morosin, *Acta Crystallogr., Sect. B: Struct. Crystallogr. Cryst. Chem.*, 1977, **33**, 2137–2143.
- M. Maekawa, M. Y. Ozawa and Y. A. Yagasaki, *Inorg. Chem.*, 2006, **45**, 9608–9609.
- R. P. Bontchev and M. Nyman, *Angew. Chem.*, 2006, **118**, 6822–6824, (*Angew. Chem., Int. Ed.*, 2006, **45**, 6670–6672).
- (a) R. Tsunashima, D. L. Long, H. N. Miras, D. Gabb, C. P. Pradeep and L. Cronin, *Angew. Chem., Int. Ed.*, 2010, **49**, 113–116; (b) P. Huang, C. Qin, Z. M. Su, Y. Xing, X. L. Wang, K. Z. Shao, Y. Q. Lan and E. B. Wang, *J. Am. Chem. Soc.*, 2012, **134**, 14004–14010.
- (a) M. Nyman, L. J. Criscenti, F. Bonhomme, M. A. Rodriguez and R. T. Cygan, *J. Solid State Chem.*, 2003, **176**, 111–119; (b) C. A. Ohlin, E. M. Villa, J. C. Fettinger and W. H. Casey, *Angew. Chem., Int. Ed.*, 2008, **47**, 5634–5636; (c) C. A. Ohlin, E. M. Villa, J. C. Fettinger and W. H. Casey, *Dalton Trans.*, 2009, 2677–2678.
- J. Niu, G. Chen, J. Zhao, P. Ma, S. Li, J. Wang, M. Li, Y. Bai and B. Ji, *Chem. – Eur. J.*, 2010, **16**, 7082–7086.

- 9 (a) G. Guo, Y. Xu, J. Cao and C. Hu, *Chem. Commun.*, 2011, **47**, 9411–9413; (b) G. Guo, Y. Xu, J. Cao and C. Hu, *Chem. – Eur. J.*, 2012, **18**, 3493–3497; (c) P. Huang, C. Qin, X. L. Wang, C. Y. Sun, G. S. Yang, K. Z. Shao, Y. Q. Jiao, K. Zhou and Z. M. Su, *Chem. Commun.*, 2012, **48**, 103–105; (d) J. H. Son, C. A. Ohlin, E. C. Larson, P. Yu and W. H. Casey, *Eur. J. Inorg. Chem.*, 2013, **10–11**, 1748–1753.
- 10 J. H. Son, C. A. Ohlin and W. H. Casey, *Dalton Trans.*, 2012, **41**, 12674–12677.
- 11 J. H. Son, C. A. Ohlin and W. H. Casey, *Dalton Trans.*, 2013, **42**, 7259–7533.
- 12 (a) H. Weiner, A. Trovarelli and R. G. Finke, *J. Mol. Catal. A: Chem.*, 2003, **191**, 253–279; (b) M. W. Droege and R. G. Finke, *J. Mol. Catal.*, 1991, **69**, 323–338.
- 13 (a) R. G. Finke and M. W. Droege, *J. Am. Chem. Soc.*, 1984, **106**, 7274–7277; (b) H. Weiner, J. D. Aiken and R. G. Finke, *Inorg. Chem.*, 1996, **35**, 7905–7913.
- 14 (a) D. A. Judd, Q. Chen, C. F. Campana and C. L. Hill, *J. Am. Chem. Soc.*, 1997, **119**, 5461–5462; (b) G. S. Kim, H. Zeng, W. A. Neiwert, J. J. Cowan, D. VanDerveer, C. L. Hill and I. A. Weinstock, *Inorg. Chem.*, 2003, **42**, 5537–5544; (c) G. S. Kim, H. Zeng and C. L. Hill, *Bull. Korean Chem. Soc.*, 2003, **24**, 1005–1008; (d) G. S. Kim, H. D. Zeng, D. VanDerveer and C. L. Hill, *Angew. Chem.*, 1999, **111**, 3413–3416, (*Angew. Chem., Int. Ed.*, 1999, **38**, 3205–3207); (e) M. K. Harrup, G. S. Kim, H. Zeng, R. P. Johnson, D. VanDerveer and C. L. Hill, *Inorg. Chem.*, 1998, **37**, 5550–5556.
- 15 (a) C. A. Ohlin, E. M. Villa, J. C. Fettinger and W. H. Casey, *Inorg. Chim. Acta*, 2010, **363**, 4405–4407.
- 16 C. A. Ohlin, E. M. Villa, J. C. Fettinger and W. H. Casey, *Angew. Chem., Int. Ed.*, 2008, **47**, 8251–8254.
- 17 V. W. Day, W. C. Klemperer and C. Schwartz, *J. Am. Chem. Soc.*, 1987, **109**, 6030–6044.
- 18 J. H. Son, J. R. Wang, F. E. Osterloh, P. Yu and W. H. Casey, *Chem. Commun.*, 2014, **50**, 836–838.
- 19 C. M. Flynn and G. D. Stucky, *Inorg. Chem.*, 1969, **8**, 178–180.
- 20 M. Filowitz, R. K. C. Ho, W. G. Klemperer and W. Shum, *Inorg. Chem.*, 1979, **18**, 93–103.
- 21 M. Nyman, T. M. Alam, F. Bonhomme, M. A. Rodriguez, C. S. Frazer and M. E. Welk, *J. Cluster Sci.*, 2006, **17**, 197–219.
- 22 S. C. Abrahams, R. L. Collin and W. N. Lipscomb, *Acta Crystallogr.*, 1951, **4**, 15–20.
- 23 S. S. Mal, M. H. Dickman and U. Kortz, *Chem. – Eur. J.*, 2008, **14**, 9851–9855.
- 24 (a) B. S. Bassil, S. S. Mal, M. H. Dickman, U. Kortz, H. Oelrich and L. Walder, *J. Am. Chem. Soc.*, 2008, **130**, 6696–6697; (b) S. S. Mal, N. H. Nsouli, M. Carraro, A. Sartorel, G. Scorrano, H. Oelrich, L. Walder, M. Bonchio and U. Kortz, *Inorg. Chem.*, 2010, **49**, 7–9; (c) Y. Sakai, Y. Kitakoga, K. Hayashi, K. Yoza and K. Nomiya, *Eur. J. Inorg. Chem.*, 2004, **23**, 4646–4652.
- 25 (a) D. Brown and D. Altermatt, *Acta Crystallogr., Sect. B: Struct. Crystallogr. Cryst. Chem.*, 1985, **41**, 244–247; (b) H. H. Thorp, *Inorg. Chem.*, 1992, **31**, 1585–1588.
- 26 (a) F. E. Osterloh, *Chem. Mater.*, 2008, **20**, 35–54; (b) Z. Zhang, Q. Lin, D. Kurunthu, T. Wu, F. Zuo, S. T. Zheng, C. J. Bardeen, X. Bu and P. Y. Feng, *J. Am. Chem. Soc.*, 2011, **133**, 6934–6937.
- 27 A. Besserguenew, M. Dickman and M. Pope, *Inorg. Chem.*, 2001, **40**, 2582–2586.
- 28 (a) G. S. Kim, H. D. Zeng, D. VanDerveer and C. L. Hill, *Angew. Chem.*, 1999, **111**, 3413–3416, (*Angew. Chem., Int. Ed.*, 1999, **38**, 3205–3207); (b) M. K. Harrup, G. S. Kim, H. Zeng, R. P. Johnson, D. VanDerveer and C. L. Hill, *Inorg. Chem.*, 1998, **37**, 5550–5556.
- 29 (a) H. Hartl, F. Pickhard, F. Emmerling and C. Rohr, *Z. Anorg. Allg. Chem.*, 2001, **627**, 2630–2638; (b) C. A. Ohlin, E. M. Villa, J. C. Fettinger and W. H. Casey, *Inorg. Chim. Acta*, 2010, **363**, 4405–4407; (c) J. Y. Piquemal, L. Salles, G. Chottard, P. Herson, C. Ahcine and J. M. Brégeault, *Eur. J. Inorg. Chem.*, 2006, **5**, 939–947.
- 30 Z. L. Wang, H. Q. Tan, W. L. Chen, Y. G. Li and E. B. Wang, *Dalton Trans.*, 2012, **41**, 9882–9884.